Available online at www.sciencedirect.com
ScienceDirect
Journal of Power Sources 173 (2007) 842–852
JOURNAL OF POWER SOURCES
www.elsevier.com/locate/jpowsour

Surface-modified Y zeolite-filled chitosan membrane for direct methanol fuel cell

Hong Wu, Bin Zheng, Xiaohong Zheng, Jingtao Wang, Weikang Yuan, Zhongyi Jiang *

Key Laboratory for Green Chemical Technology, School of Chemical Engineering and Technology, Tianjin University, Tianjin 300072, China

Received 17 July 2007; received in revised form 9 August 2007; accepted 9 August 2007
Available online 15 August 2007

Abstract

Hybrid membranes composed of chitosan (CS) as organic matrix and surface-modified Y zeolite as inorganic filler are prepared and their applicability for DMFC is demonstrated by methanol permeability, proton conductivity and swelling property. Y zeolite is modified using silane coupling agents, 3-aminopropyl-triethoxysilane (APTES) and 3-mercaptopropyl-trimethoxysilane (MPTMS), to improve the organic–inorganic interfacial morphology. The mercapto group on MPTMS-modified Y zeolite is further oxidized into sulfonic group. Then, the resultant surface-modified Y zeolites with either aminopropyl groups or sulfonicpropyl groups are mixed with chitosan in acetic acid solution and cast into membranes. The transitional phase generated between chitosan matrix and zeolite filler reduces or even eliminates the nonselective voids commonly exist at the interface. The hybrid membranes exhibit a significant reduction in methanol permeability compared with pure chitosan and Nafion117 membranes, and this reduction extent becomes more pronounced with the increase of methanol concentration. By introducing $-SO_3H$ groups onto zeolite surface, the conductivity of hybrid membranes is increased up to 2.58×10^{-2} S cm^{-1}. In terms of the overall selectivity index ($\beta = \sigma/P$), the hybrid membrane is comparable with Nafion117 at low methanol concentration (2 mol L^{-1}) and much better (three times) at high methanol concentration (12 mol L^{-1}).

Keywords: Chitosan; Zeolite; Silane coupling agent; Hybrid membrane; Methanol permeability; Proton conductivity

1. Introduction

Direct methanol fuel cell (DMFC), as a novel energy conversion device, is attractive for transportation and portable power generator applications due to its high energy density, simplified system design, convenient storage, recharge and transport of fuels [1]. Polyperfluorosulfonic acid ionomer initially developed by DuPont and successfully used in H_2/O_2 fuel cell, Nafion^{TM}, is currently the most commonly utilized proton exchange membrane (PEM) for DMFCs because of its superior chemical stability and high proton conductivity. However, one of the main drawbacks of the Nafion^{TM} series membranes is the severe methanol crossover from anode to cathode, resulting in not only a serious reduction in the cell efficiency caused by methanol–oxygen mixed potential at the cathode, but also a considerable decease in fuel utilization efficiency [2,3]. Alternative PEMs with low methanol permeability and high proton conductivity as well as low swelling, low cost and low toxicity are certainly expected for DMFC exploitation.

Reduction of methanol crossover through PEMs can be achieved by two routes: rational selection or invention of membrane materials, and appropriate manipulation of membrane morphology [4–6]. If a methanol-rejecting and proton conducting DMFC membrane could be viewed as a $H^+(H_2O)$/methanol separation media, membrane materials with excellent alcohol/water separation ability would be considered as appropriate candidates. As a matter of fact, in the field of membrane pervaporation for dehydration of alcohols, many hydrophilic polymers, such as chitosan and polyvinyl alcohol, have been widely used due to their preferential affinity towards water [7–9]. Chitosan is a polysaccharide prepared by the deacetylation of chitin that mainly obtained from the crab and shrimp shells [10]. Due to the inherent characteristics such as hydrophilicity, biocompatibility, antibacterial properties, remarkable affinity towards certain substances and facile film formation, chitosan has been grad-

* Corresponding author. Tel.: +86 22 27892143; fax: +86 22 27892143.
E-mail address: zhyjiang@tju.edu.cn (Z. Jiang).

0378-7753/$ – see front matter © 2007 Elsevier B.V. All rights reserved.
doi:10.1016/j.jpowsour.2007.08.020

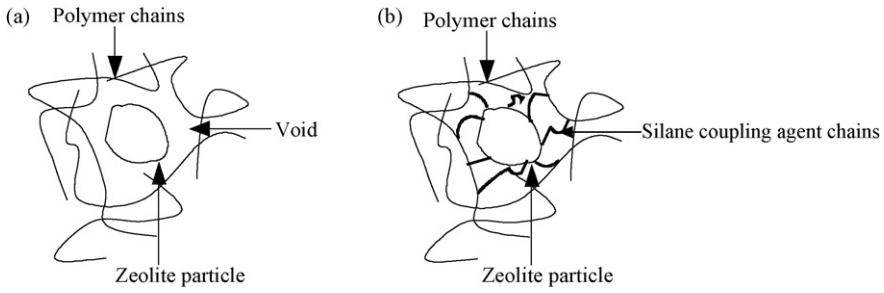

Fig. 1. Schematic illustration of polymer-filled interfacial morphology: (a) voids and (b) transitional phase at interface.

ually regarded as a kind of promising material for membrane fabrication.

Herein, chitosan is chosen as the polymer matrix considering its excellent alcohol-rejecting performance. However, in its normal state, chitosan film has very low conductivity and high degree of swelling [11]. Serious swelling would induce disentanglement within the polymer matrix, thus facilitating the permeation of methanol and water as well as that of the proton to some extent [12,13], resulting in a loss of $H^+(H_2O)$/methanol selectivity. To reduce the swelling degree, chitosan was usually either cross-linked with sulfuric acid or other polyelectrolytes [14,15], or incorporated with some inorganic particles such as silica, zeolites, zirconia and montmorillonite [16–19]. Among these inorganic particles, zeolite, unique for its molecular sieving effect, is attracting considerable research interest due to its well-defined open crystal structures with a pore size of several angstroms, low cost and flexible configurations.

For polymer–zeolite hybrid membranes, the membrane morphology and polymer–inorganic interfacial property are crucial to methanol permeation [20]. Researchers found that when the polymer is in glassy state under preparation or application conditions, nonselective or less selective voids are often present at the interface between the polymer phase and the external surface of zeolite as shown in Fig. 1(a) [21–23]. It is thus reasonable to expect a reduction in methanol crossover by improving the interfacial morphology. In a previous study, plasticizer was used to enhance the polymer–inorganic compatibility by increasing the polymer (chitosan) chain flexibility and thus reducing the stress arisen during the membrane formation process [24]. In this study, another approach involving zeolite surface modification was introduced in hope to create an additional transitional phase between polymer and inorganic phase as schematically illustrated in Fig. 1(b). Two functional organotriethoxysilanes either with –SH or $–NH_2$ groups were selected as the modifiers due to their capability of co-condensing with the hydroxyl groups on zeolite surface. Some studies have confirmed the effectiveness of use of silane coupling reagents in membrane preparation for separation and DMFC [25–29]. Sulfuric acid was used as an effective cross-linker for chitosan matrix to prohibit its excess swelling and, meanwhile, to protonate the amino groups on chitosan, endowing the polymer with higher conductivity. In addition, to further increase the membrane conductivity, mercaptosilane-modified zeolite was further oxidized to attach additional $–SO_3H$ groups and then incorporated into chitosan bulk to fabricate the membranes. The chemical and physical properties of the hybrid membranes were characterized and their methanol permeability and proton conductivity were thoroughly investigated.

2. Experimental

2.1. Materials and chemicals

Chitosan (CS) with a degree of deacetylation of 91% was supplied by Zhejiang Golden-shell Biochemical Co. Ltd. NaY zeolite with a Si/Al ratio of 2.50 was purchased from Shanghai Xinnian Shihua Co. Ltd. 3-Aminopropyl-triethoxysilane (APTES) and 3-mercaptopropyl-trimethoxysilane (MPTMS) were purchased from Power Chemical Corporation. Acetic acid, sulfuric acid and methanol were purchased locally. De-ionized water was used throughout the study.

2.2. Surface modification of NaY zeolite

Surface modification of NaY zeolite by organotriethoxysilane was carried out according to the procedure described in the literature [30]: NaY zeolite (1.4 g) and NH_4NO_3 aqueous solution (700 mL, 1 mol L^{-1}) were mixed under stirring at 80 °C for 12 h. The zeolite was then filtered and rinsed with de-ionized water till electric neutrality and dried at room temperature followed by calcination at 500 °C for 6 h to fully convert NaY into HY form.

HY zeolite, APTES and toluene (mass ratio 1:2:20) were refluxed under stirring at 110 °C for 24 h. The zeolite was filtered and rinsed with both ethanol and water to remove the silane residues. The resulting APTES-modified zeolite was dried and denoted as H_2NY zeolite.

For MPTMS-modified zeolite, the above-mentioned procedure was followed except that MPTMS was used instead of APTES. The resulting zeolite with –SH groups, denoted as HSY, was further oxidized at 25 °C in 30 wt.% H_2O_2 solution for 24 h to convert the –SH groups into $–SO_3H$ groups (HO_3SY zeolite).

2.3. Membrane preparation and pretreatment

Chitosan was dissolved in 2 wt.% aqueous acetic acid to acquire a 2 wt.% concentration by stirring at 80 °C. A desired amount of zeolite was then added to the above solution and stirred at 80 °C for 2 h followed by dispersion under ultrasonic for 1 h. After filtration and degasification, the resulting homoge-

nous solution was cast onto a clean glass plate and dried at 25 °C. Next, the membrane was immersed and cross-linked in 2 mol L^{-1} H_2SO_4 solution for 24 h and rinsed with de-ionized water. Finally, the membrane was dried at 25 °C under vacuum. Pure chitosan membrane and NaY-, H_2NY- and HO_3SY-filled chitosan membranes were prepared and designated, respectively, as CS, CS–NaY(X), CS–H_2NY(X) and CS–HO_3SHY(X) henceforth where X represents the mass content of zeolite.

Nafion117 membrane, used as a reference, was pretreated in boiling water, 3wt.% H_2O_2, 1 mol L H_2SO_4 and boiling water, alternatively, each for 1 h, to completely remove the impurities and fully convert the membrane into H^+-form.

Prior to both permeability and conductivity measurements, the membranes were equilibrated in de-ionized water.

2.4. Characterizations

The elemental composition and state on the zeolite surface before and after modification was compared using X-ray photoelectron spectroscopy (XPS, PHI 1600, Mg Kα X-ray source for excitation).

Nitrogen adsorption–desorption measurements were carried out using a Micromeritics Gemini V instrument to compare the BET surface area, total pore volume and pore size between the unmodified and modified zeolites.

The FT-IR spectra (4000–400 cm^{-1}) of zeolite before and after surface modification and CS, CS–NaY, CS–H_2NY and CS–HO_3SY membranes were recorded using a Nicolet-740, Perkin-Elmer-283B FT-IR Spectrometer.

The crystalline structures of different zeolites and membranes were investigated with a RigakuD/max2500v/pa X-ray diffractometer (CuK 40 kV, 200 mA). The peak position and area were extracted with MDIjade5 software.

The morphology of pure chitosan and hybrid membranes was observed by scanning electron microscopy (SEM, Philips XL30ESEM). Membrane samples were freeze-fractured in liquid nitrogen and sputtered with gold.

2.5. Water uptake, methanol solution uptake and swelling property

The water uptake and methanol–water solution uptake of the hybrid membranes were determined by measuring the membrane weight difference before and after immersion. Membrane samples were dried under vacuum at 25 °C for 24 h and weighted (W_{dry}) before being immersed in de-ionized water or 50 wt.% methanol–water solution at room temperature for 24 h. The wet membrane was wiped with blotting paper to remove residual water from the surface and weighed (W_{wet}). The uptake was calculated by the following equation:

$$\text{uptake}\,(\%) = \frac{W_{wet} - W_{dry}}{W_{dry}} \times 100$$

The swelling property was determined by measuring the area change of the membrane upon equilibrating the membranes in water at room temperature for 24 h. The swelling ratio was calculated by the following equation:

$$\text{swelling}\,(\%) = \frac{A_{wet} - A_{dry}}{A_{dry}} \times 100$$

where A_{dry} and A_{wet} are the areas of the dry and wet samples, respectively.

2.6. Ion exchange capacity (IEC)

Ion exchange capacity of the membrane was determined by a titration method. The membranes in H^+ form were immersed in 20 mL of NaCl saturated aqueous solution under continuous stirring for 24 h to liberate H^+. The released amount of H^+ in the solution was back titrated with 0.01 mol L^{-1} NaOH solution. The ion exchange capacity (IEC, mmol g^{-1}) was calculated by:

$$\text{IEC} = \frac{0.01\text{Vol}_{NaOH}}{W_d}$$

where Vol_{NaOH} is the volume of NaOH (L) consumed in titration and W_d (g) is the weight of the dry membrane sample.

2.7. Proton conductivity

The proton conductivity of the membranes in the transverse direction was measured in two-point-probe conductivity cells by the ac impedance spectroscopy method over a frequency range of 1–10^6 Hz with oscillating voltage of 10 mV, using a frequency response analyzer (FRA, Autolab PGSTST20). Prior to measurement, the membrane sample was equilibrated in 0.2 mol L^{-1} H_2SO_4 for 24 h and then placed between two stainless steel electrodes. The proton conductivity (σ, S cm^{-1}) of the membrane was calculated by $\sigma = d/RA$, where d and A are the thickness and the testing area of the membrane sample, respectively, and R is the membrane resistance derived from the low intersect of the high frequency semicircle on a complex impedance plane with Re (z) axis.

2.8. Methanol permeability

The methanol permeability was determined using a diaphragm diffusion cell [31]. The cell consists of two compartments with identical volume separated by the membrane sheet. Compartment A was initially filled with a solution of methanol and compartment B with de-ionized water. Both compartments were well stirred during the test. The methanol concentration in compartment B was determined using a gas chromatography (Agilent 6820) equipped with a TCD detector and a DB624 column. The methanol permeability (P, cm^2 s^{-1}) was calculated as follows:

$$P = \frac{kVL}{SC_{A_0}}$$

where k is the slope of the curve plotted by concentration in compartment B versus time, V the volume of the compartment, S and L the membrane area and thickness, respectively and C_{A_0} is the initial concentration of methanol in compartment A.

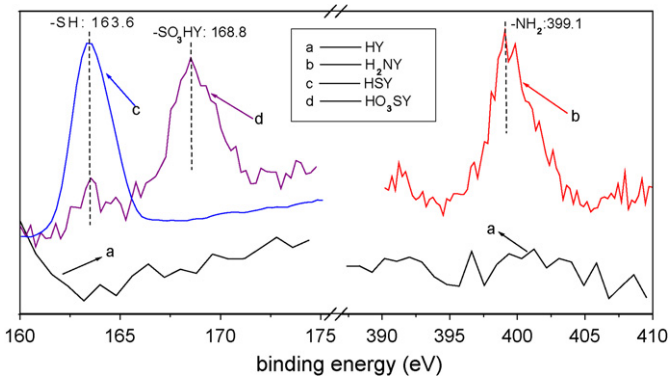

Fig. 2. XPS spectra of zeolite surface before and after modification.

3. Results and discussions

3.1. Characterization of zeolite before and after modification

XPS spectra of zeolite before and after surface modification are presented in Fig. 2. Compared with HY zeolite in the binding energy range of 390–410 eV (Fig. 2(a) right), a new peak clearly appears at 399.1 eV after APTES-modification (Fig. 2(b)) which attributes to the nitrogen element in the $–NH_2$ group and confirms the successful mercaptosilane grafting. The mass content of nitrogen on the surface of APTES-modified zeolite calculated from XPS data is 2.5%. In the case of MPTMS-modification, compared with the spectrum of the HY zeolite in the range of 165–175 eV (Fig. 2(a) left), a new intensive peak at 163.6 eV which attributes to the sulfur element in –SH group can be clearly observed (Fig. 2(c)). After further oxidation in H_2O_2, the intensity of the peak at 163.6 eV is remarkably decreased while another new peak at 168.8 eV, which is attributed to the sulfur in $–SO_3H$ group, appears (Fig. 2(d)) and increases with the increase of oxidation time (data not shown). After 24 h oxidation, the total mass content of sulfur is 2.50%, of which 2.37% comes from $–SO_3H$ groups, indicating that 94.8% –SH groups has been oxidized into $–SO_3H$.

Table 1
BET surface area, total pore volume and pore size of zeolites

	NaY	NH_2Y	SO_3HY
Surface area ($m^2\ g^{-1}$)	328.1	168.3	72.8
Total pore volume ($cm^3\ g^{-1}$)	0.156	0.061	0.027
Pore size (nm)	0.674	0.450	0.464

The surface area, total pore volume and pore size of zeolites are listed in Table 1. A noticeable reduction in all the above three values after the modification indicates that the condensation between the silanol groups and the hydroxyl groups on zeolite surface indeed blocks the zeolite pores to certain extent. This blockage effect becomes more pronounced in the case of SO_3HY zeolite than NH_2Y zeolite, probably due to the further intra- and inter-molecule condensation during the oxidation process. The decreased pore size, still big enough for free transport of water and proton, is supposed to be a favorable factor for methanol barrier performance.

3.2. Membrane formation and morphology

The compatibility between the polymer and the surface of the inorganic filler is a key issue in determining the final membrane property and performance. To improve the interfacial morphology in hybrid membrane, a transitional phase is expected to be created between the organic and inorganic phases, mitigating or eliminating the nonselective voids. In this study, functional organosilanes were used to modify the zeolite surface and create the desired transitional phase. The aryloxy groups (RO–, R=CH_3 or CH_3CH_2) at one end of the silane can be hydrolyzed into silanol groups (Si–OH) and then co-condensed with the hydroxyl groups (–OH) on the zeolite surface. The functional groups ($H_2N–(CH_2)_3–$ in APTES, $HS–(CH_2)_3–$ in MPTMS) can render the zeolite desirable surface properties. As illustrated in Fig. 3, after modification, the organosilane “arms”

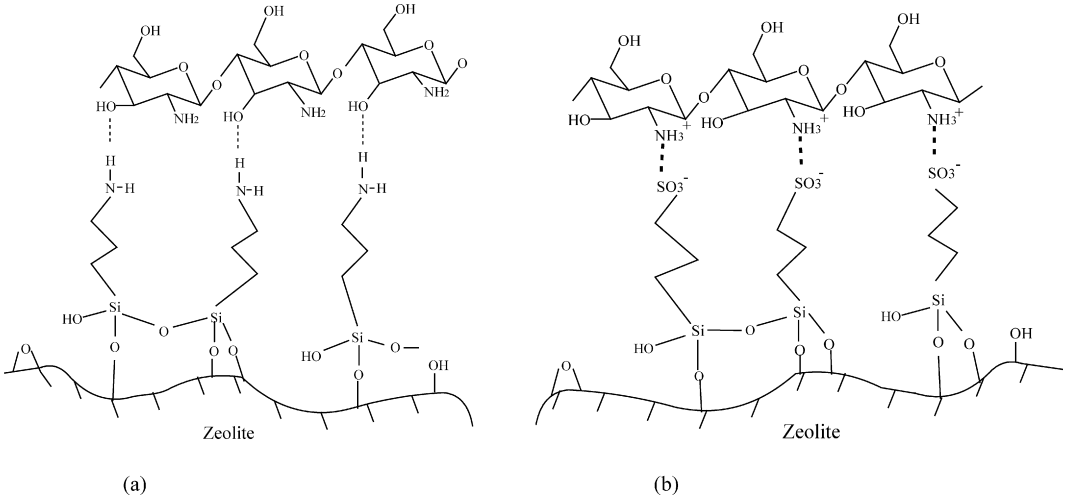

Fig. 3. Schematic illustration of interfacial interaction existed in modified-zeolite-filled chitosan membranes (a) CS–H_2NY membranes and (b) CS–HO_3SY membranes.

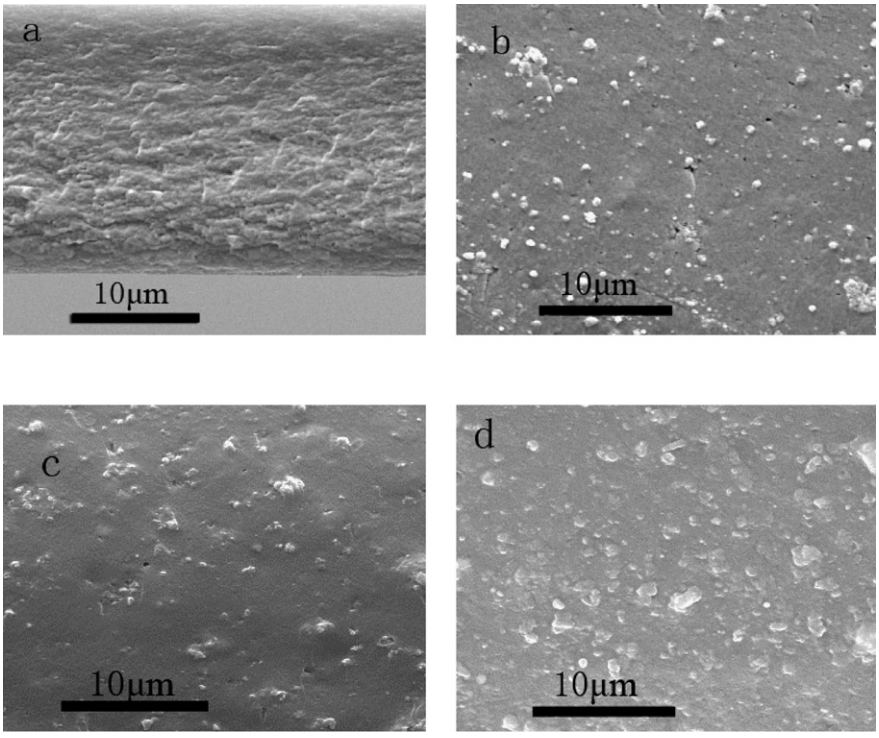

Fig. 4. Cross-section SEM images of pure chitosan and zeolite-filled chitosan membranes. (a) Chitosan, (b) CS–NaY (20%), (c) CS–H_2NY (20%) and (d) CS–HO_3SY (20%)

(–CH_2–CH_2–CH_2–Si≡) were grafted onto the zeolite surface with specific functional groups (–NH_2 or –SO_3H) linked to at the end of these "arms" like "hands". When these modified zeolite were blended with the rigid glassy chitosan, the –NH_2 or –SO_3H groups were expected to grasp the polymer chains around them via hydrogen bonds or acid-base ionic interaction formed with the –OH and –NH_2 groups on chitosan. Thus, a transitional phase with a somewhat flexibility due to the propyl chains was generated, leading to a better compatible interface.

Fig. 4 presents the cross-section SEM images of chitosan and hybrid membranes. While the pure chitosan membrane shows a void-free dense structure (Fig. 4(a)), voids around the unmodified NaY zeolite particles can be clearly observed in the CS–NaY (20%) hybrid membrane (Fig. 4(b)). Much better interfacial morphology was obtained after zeolite modification as shown in Fig. 4(c) and (d), confirming an improvement in compatibility between the organic polymer and inorganic filler by means of silane modification. It should be mentioned that, the CS–HO_3SY hybrid membrane displays better interfacial morphology than CS–H_2NY hybrid membrane.

3.3. FT-IR spectra

The FT-IR spectra of Y zeolite before and after modification and that of chitosan and zeolite-filled chitosan membranes are shown in Fig. 5 and Fig. 6, respectively. The framework infrared spectrum of NaY is in good agreement with the data reported in literature [32]. The bands at 1049 cm^{-1} (υ_{as}), 723 cm^{-1} (υ_s) and 457 cm^{-1} (T–O band) are assigned to the three lattice modes associated with internal vibrations of the (Si, Al) O_4 tetrahedral unites which designated as TO_4 in the framework of Y zeolite and are structure-insensitive. The structure-sensitive vibrations due to external linkages between tetrahedrals are found at 1158 cm^{-1} (υ_{as}), 795 cm^{-1} (υ_s) and 580 cm^{-1} (double six-rings). A characteristic strong and broad band at around 3440 cm^{-1} corresponds to O–H stretching vibrations of the hydroxyl groups. No obvious changes in the characteristic wavelength range of Y zeolite (450–1500 cm^{-1}) are observed, indicating that the framework chemical structure remains unchanged after modification. The intensity of the band at 3440 cm^{-1} decreases notably after silane modification as a result of the consumption of the zeolite hydroxyl groups by condensing with the silanol groups. The distinct peaks of the

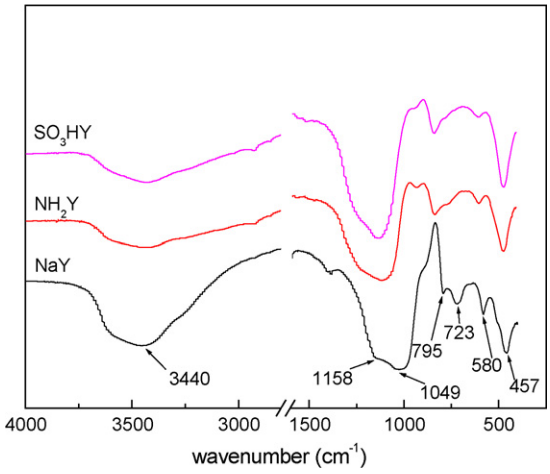

Fig. 5. FT-IR spectra of Y zeolite before and after modification.

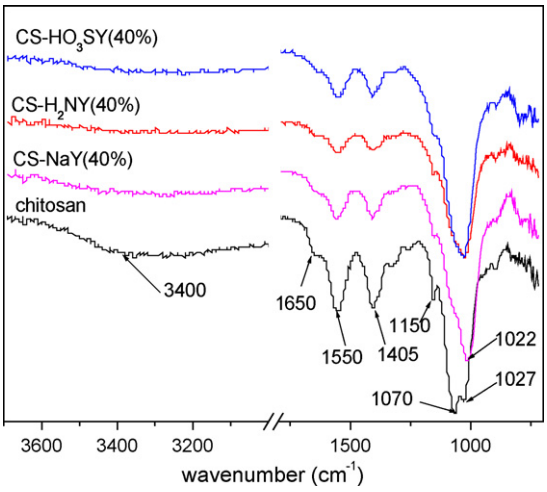

Fig. 6. FT-IR spectra of chitosan membrane and zeolite-filled chitosan membranes.

sulfonic group (1420–1310 cm^{-1} and 1235–1145 cm^{-1}) [33] attributing, respectively, to the asymmetric and symmetric SO_2 stretching vibration bands can not be discriminated because they are overlapped with the peaks of TO_4.

For pure chitosan membrane, the characteristic bands at 3400 cm^{-1}, 1650 cm^{-1} and 1550 cm^{-1} are attributed to hydroxyl group, amide I and amide II groups, respectively. The bands at 1070 cm^{-1}, 1380 cm^{-1} and 1160 cm^{-1} are due to the C–O stretching, $–CH_2$ bending and asymmetric stretching of C–O–C [34]. The band at 1150 cm^{-1} attributes to the symmetric vibration band of S=O=S. The intensity of the bands at 3400 cm^{-1}, 1650 cm^{-1} and 1550 cm^{-1} decreases in the hybrid membrane spectrum because of the interaction between the –OH, $–NH_2$ groups on chitosan and the –OH, $–NH_2$ and $–SO_3H$ groups on zeolite. The two bands at 1070 cm^{-1} and 1027 cm^{-1} in the pure chitosan membrane merge into one and shift to 1022 cm^{-1} in the zeolite filled membranes due to the overlapping of Si–O band with the C–O stretching band.

3.4. XRD analysis

Fig. 7(a) shows the XRD patterns of Y zeolite before and after modification. It can be seen that the surface-modified zeolite keeps the identical characteristic peaks with the unmodified NaY zeolite, which suggests that the surface-modified zeolite display the same crystalline structure with the original NaY zeolite. After surface modification, some characteristic peaks of zeolite become weaker, and an obvious amorphous crystalline structure appears at 15–30° which is due to the presence of grafted silane coupling agent chains on the zeolite surface.

According to Chen et al. [35], chitosan has two crystal forms: form I has the major crystalline peaks at 11.2° and 18.0°, while

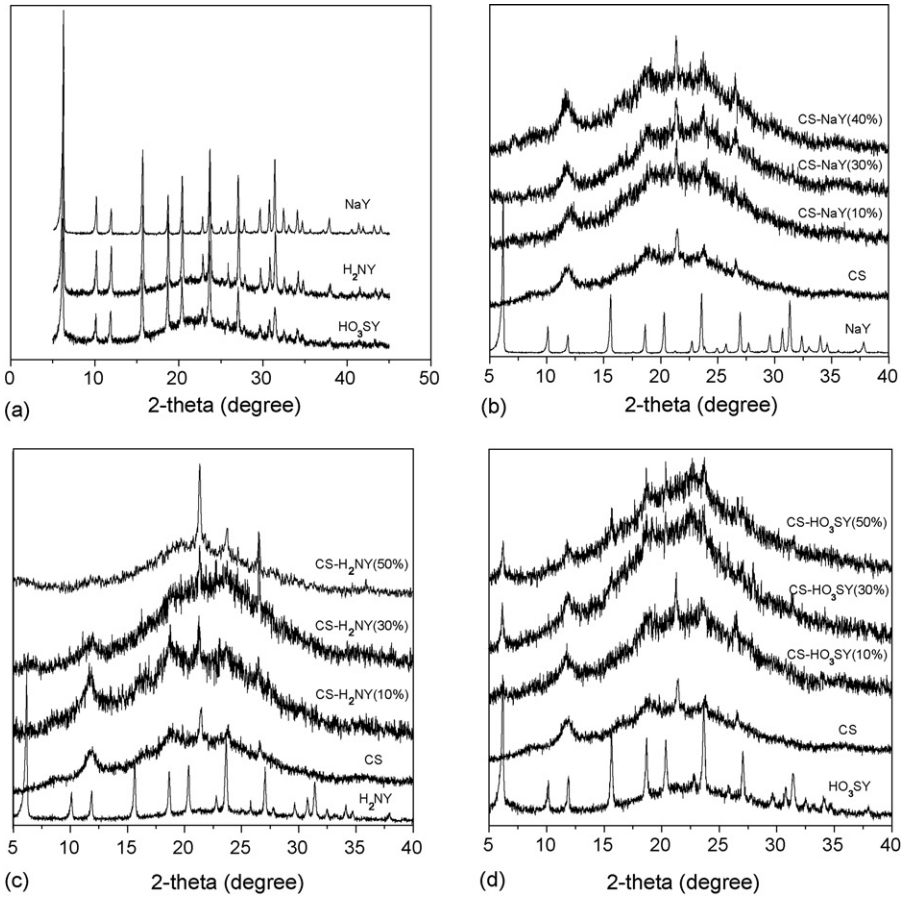

Fig. 7. XRD patterns of zeolite and zeolite-filled chitosan membranes (a) Y zeolite before and after modification, (b) CS–NaY hybrid membranes (c) CS–H_2NY hybrid membranes and (d) CS–HO_3SY hybrid membranes.

form II has major peaks at 20.9° and 23.8°. The chitosan membrane prepared in this work seems to contain both of the two crystal forms: form I (11.5°, 18.8°) and form II (21.5°, 23.9°) as shown in Fig. 7(b). The broad peak appears at around 20° is attributed to the partly crystallized polymer chains. It can be seen from Fig. 7(b) and (d) that the intensity of the characteristic chitosan crystal peaks decrease with the increase of zeolite content. This indicates that zeolite surface modification enhances the interaction between zeolite and chitosan matrix and destroys the interaction among chitosan molecules. In CS–HO_3SY membranes, the amorphous crystalline peak at 15–30° becomes narrower and stronger with increasing the HO_3SY content. This might be explained that the stronger interaction between the $–SO_3H$ on the zeolite and the $–NH_2$ on the chitosan destroys the original crystal structure of chitosan, and reconstructs into a more ordered structure which may lead to a better separation performance.

3.5. Membrane water uptake, methanol uptake and swelling

Fig. 8 shows the water uptake and methanol solution uptake of the hybrid membranes. In this study, 50 wt.% methanol/water solution uptake of hybrid membranes was measured. Both the water uptake and methanol solution uptake of hybrid membranes decrease with the increase of zeolite content. This is attributed to the addition of the zeolite particles that are less hydrophilic than the chitosan polymer and also to the rigidification of polymer chains caused by the filling of inorganic particles. When the zeolite content is lower than 30%, the water uptake and methanol solution uptake of CS–NaY membranes is higher than that of pure chitosan membrane. Our previous work has confirmed that the unselective voids exist at the interface of organic matrix and inorganic particles increase the free volume of chitosan membrane and thus more water or methanol can be stored in these voids [24]. Under the same zeolite content, the water uptake of different hybrid membranes follows such order: CS–NaY > CS–H_2NY > CS–HO_3SY. The decrease trend of the water uptake for modified-zeolite-filled membrane is owing to

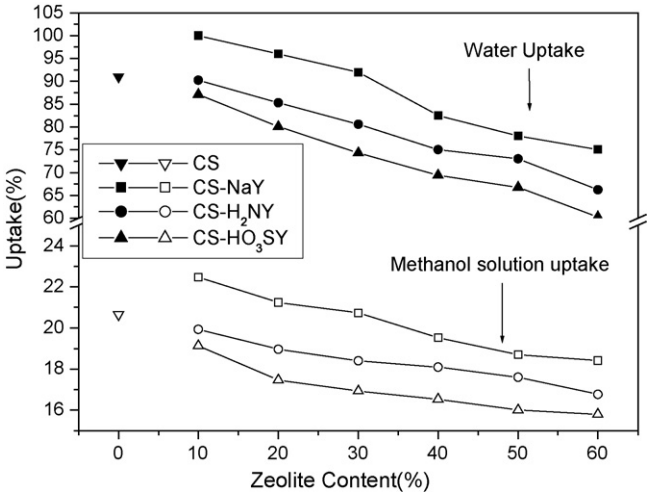

Fig. 8. Water uptake and methanol solution uptake of zeolite-filled chitosan membranes.

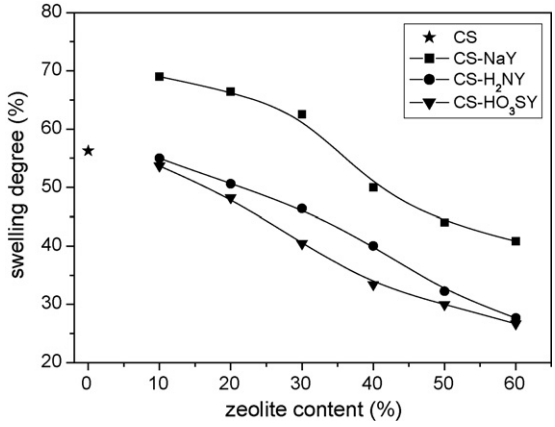

Fig. 9. Swelling degree of zeolite-filled chitosan membranes.

that the surface modification of zeolite strengthens the adhesion between the polymer and the zeolite particle, thus generating a void-less or void-free structure. Comparing the water uptake data and methanol solution uptake data, it can be seen that the water uptake of hybrid membranes is much higher than the methanol solution uptake of hybrid membranes with the same zeolite content, indicating that hybrid membranes have priority to adsorb water molecules over methanol molecules.

For chitosan membrane, methanol crossover depends greatly on the membrane swelling, and obviously, low swelling degree is favorable for hindering methanol permeation. As shown in Fig. 9, the swelling degree was significantly lowered by the addition of modified zeolites. The possible reason may be that incorporation of inorganic components and the transitional phase generated between the polymer matrix and inorganic particle effectively restrict the stretching of the polymer chain in aqueous solution.

3.6. Ion exchange capacity (IEC)

Ion exchange capacity (IEC) is an indirect and reliable approximation of the proton conductivity [14]. The IEC values of all the membranes prepared in this study are listed in Table 2. The pristine chitosan shows an IEC value of 0.174 mmol g^{-1}, much lower than that of Nafion117 membrane (0.886 mmol g^{-1}). The IEC values of zeolite-filled hybrid membranes are slightly lower than that of chitosan membrane and decrease with increasing zeolite content. Compared with unmodified NaY-filled CS–NaY membrane and APTES-modified H_2NY-filled CS–H_2NY membrane, CS–HO_3SY hybrid membranes show higher IECs due to the presence of additional $–SO_3H$ groups on zeolite.

3.7. Methanol permeability

Fig. 10 shows the methanol permeability as a function of methanol concentration for zeolite-chitosan hybrid membrane, chitosan membrane and Nafion117 membrane. One notable observation is that the methanol permeability of Nafion117 is much higher than that of chitosan membranes, confirming the appropriate choice of chitosan as an excellent methanol barrier. Furthermore, that the methanol permeability of Nafion

Table 2
IEC values (mmol g^{-1}) of Nafion117, chitosan and zeolite-filled chitosan hybrid membranes

Membrane	Zeolite content						
	0 (%)	10 (%)	20 (%)	30 (%)	40 (%)	50 (%)	60 (%)
Nafion117	0.886						
CS	0.174						
CS–NaY		0.106	0.098	0.102	0.096	0.092	0.094
CS–NH_2Y		0.115	0.111	0.101	0.106	0.098	0.105
CS–SO_3HY		0.168	0.159	0.147	0.140	0.152	0.133

increases with the increase of methanol concentration makes Nafion an even poorer methanol barrier at higher methanol concentrations. Chitosan and zeolite-filled chitosan membranes show just a completely reverse trend, that is, the higher the methanol concentration is, the better methanol-rejecting ability the chitosan-based membranes exhibit. The difference in the chemical and physical structure between Nafion and chitosan can account for this distinct difference in methanol permeation behavior.

After incorporating Y zeolites into chitosan, the methanol permeability was further decreased. This decrease may be attributed to the following two reasons: (1) the dispersion of inorganic particles increase the methanol permeation path length and tortuosity while the strong hydrophilic nature of Y zeolite (Si/Al = 2.50) presents much more priority for water molecules traveling through the pores; (2) the incorporation of the rigid zeolite causes local rigidification of chitosan matrix and compresses the volumes between polymer chains, thus reducing the membrane swelling and methanol uptake.

The effect of zeolite modification on the methanol barrier property can also be clearly found. Compared with the CS–NaY membrane, the silane chains grafted on zeolite particles in CS–H_2N and CS–HO_3SY membranes enhanced the compatibility between zeolite and polymer. The transitional phase created at the inorganic-polymer interface fills up the small voids and connects the two phases much closer. The reduction in zeolite pore size and total pore volume after modification is another favorable factor in increasing the water/methanol selectivity. Comparing the two modification treatments, CS–HO_3SY membrane shows a little better methanol-rejecting performance because the –SO_3H groups on the modified zeolite surface can form stronger interactions with the –NH_2 groups of chitosan than in the case of –NH_2 modification. The methanol permeability of different kinds of the hybrid membranes with same zeolite content decreases in the following order: CS–NaY > CS–H_2NY > CS–HO_3SY.

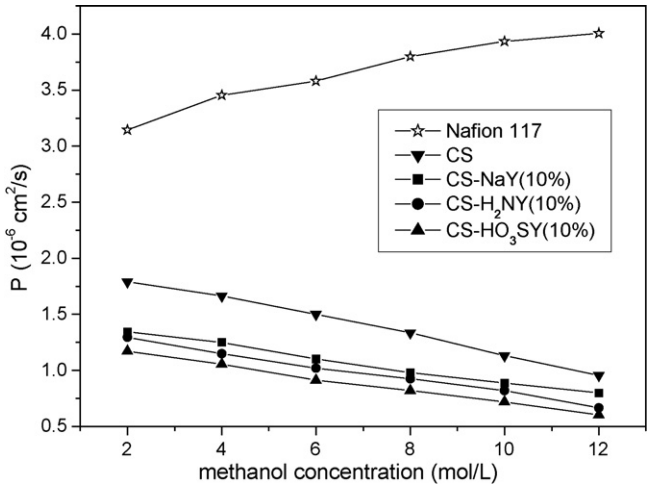

Fig. 10. Methanol permeability of membranes vs. methanol concentration.

Fig. 11 shows the methanol permeability as a function of zeolite content for zeolite-filled chitosan membranes at different methanol concentrations (2 mol L^{-1} and 12 mol L^{-1}). The methanol permeability of the hybrid membranes decreases with the increase of zeolite content when the zeolite content is less than 40%, and reaches the lowest at zeolite content of 40% for all hybrid membranes. The decrease trend is consistent with the assumption that methanol molecules preferentially move through the polymer phase while passing around the inorganic particles. At the methanol concentration of 2 mol L^{-1}, the CS–HO_3SY (40%) shows a methanol permeability of 9.04×10^{-7} cm^2 s^{-1}, less than 1/3 of that of Nafion117 under the identical condition. When the methanol concentration is increased to 12 mol L^{-1}, the methanol permeability of CS–HO_3SY (40%) is further reduced to 3.90×10^{-7} cm^2 s^{-1}, less than 1/10 of that of Nafion117. The methanol permeability increases with the increase of zeolite content higher than 40% due to the nonuniform dispersion and aggregation of zeolite particles in the membrane.

3.8. Proton conductivity

The proton conductivity of membranes synthesized in this study is listed in Table 3 and compared with Nafion117. The proton conductivity of Nafion117 has been reported in many references [36–38], but the data are not always in consistency due to different test methods and conditions. In our test, Nafion117 (full hydration) shows a proton conductivity of 6.91×10^{-2} S cm^{-1} while the pure cross-linked chitosan membrane (full hydration) shows a proton conductivity of 2.61×10^{-2} S cm^{-1}. Although the proton conductivity of hybrid membranes decreases with the increasing of zeolite content, it still can keep at an acceptable level (>1.5×10^{-2} S cm^{-1}). The proton conductivity of CS membrane mainly attributes to the high content of –NH_2 and –OH groups in the polymer. The proton transport in chitosan may occur in two mechanisms [14,6,39,40]. The first is by Grotthus or "jump" mechanism, according to which the protons pass down the –OH groups or the ionic cross-linking SO_4^{2-} and –NH_3^+

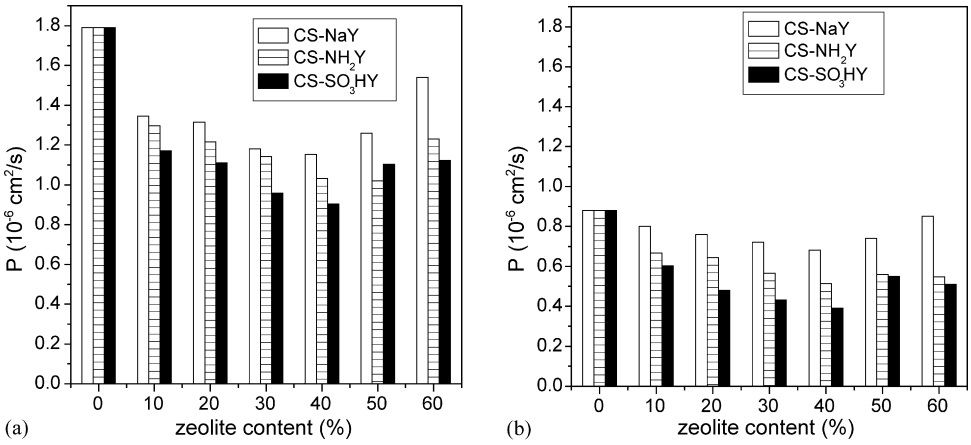

Fig. 11. Methanol permeability of zeolite-filled chitosan membranes vs. zeolite content at methanol concentration of (a) 2 mol L^{-1} and (b) 12 mol L^{-1}.

Table 3
Proton conductivity ($\times 10^{-2}$ S cm^{-1}) of Nafion117, chitosan and zeolite-filled hybrid membranes

Membrane	Zeolite content						
	0 (%)	10 (%)	20 (%)	30 (%)	40 (%)	50 (%)	60 (%)
Nafion117	6.91						
CS	2.61						
CS–NaY		2.30	2.13	1.91	1.91	1.77	1.70
CS–H_2NY		2.09	1.94	1.75	1.61	1.51	1.63
CS–HO_3SY		2.58	2.39	2.12	2.07	1.90	1.94

groups by jumping from on site to another [40]. The second is called a vehicle mechanism, assuming that the protons transfer in the form of complex like H_3O^+ or $CH_3OH_2^+$ by combining with the solvent molecules. Therefore, the vehicle mechanism is highly dependent on the amount of water or methanol molecules in the membrane. In this study, incorporation of zeolite significantly reduces the water uptake and methanol uptake of chitosan membrane, thus decreasing the proton conductivity to a certain extent. For CS–HO_3SY hybrid membrane, the –SO_3H groups interact with –NH_2 groups, the resulting –SO_3^- and –NH_3^+ reduce the energy barrier to the proton transport [40,41], leading to an increase in proton conductivity. In particular, CS–HO_3SY (10%) membrane shows conductivity as high as 2.58 S cm^{-1} which is comparable with acid cross-linked pure chitosan membrane. It is reasonable to believe that an even higher conductivity can be obtained if more –SO_3H groups are grafted on the zeolite surface, and this investigation is under further exploration.

3.9. Selectivity ($\beta = \sigma/P$)

In membrane separation processes, the efficiency for separating two components is usually evaluated by selectivity that is defined as the ratio of the permeation flux of the two components. In DMFC application, the H^+/methanol selectivity can be expressed in the form of $\beta = \sigma/P$, i.e., the ratio of proton conductivity to methanol permeability. The expression of β can be deduced from Nernst–Plank equation and Fick's law which describes the proton flux and the methanol flux, respectively [42]. In general, membranes with higher selectivity are more desirable for DMFCs [17,40]. Fig. 12 shows the selectivity of Nafion117, pure CS and zeolite-filled chitosan membranes (zeolite content 10%), which is based on their conductivities and methanol permeability measured at room temperature. The selectivity of Nafion117 decreases gradually with the increase of methanol concentration while the chitosan-based membranes prepared in this study exhibit a reverse trend, that is, the selectivity becomes increased at higher methanol concentrations due to the better methanol barrier performance of chitosan. The chitosan membrane, CS–NaY (10%) membrane and CS–H_2NY (10%) membrane exhibit higher selectivity than Nafion117 at

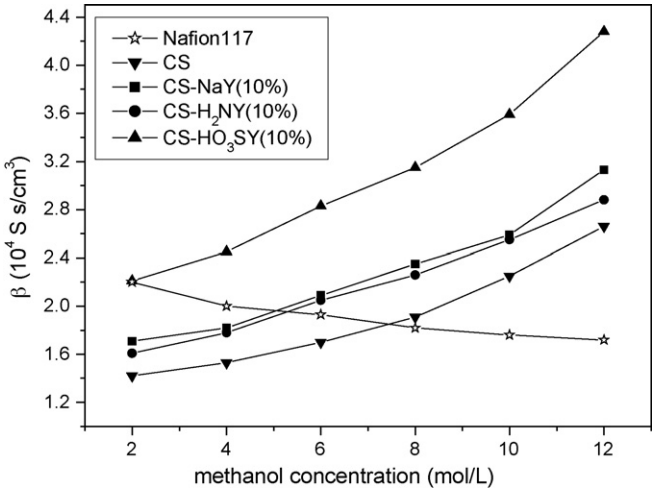

Fig. 12. Selectivity vs. methanol concentration.

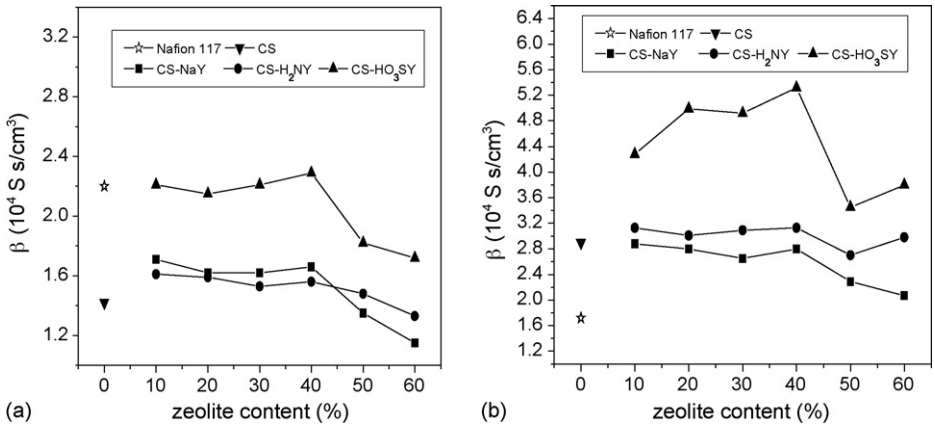

Fig. 13. Selectivity of zeolite-filled chitosan membranes vs. zeolite content at methanol concentration of (a) 2 mol L^{-1} and (b) 12 mol L^{-1}.

higher methanol concentration (>6 mol L^{-1}). In particular, the CS–SO_3HY (10%) membrane shows a comparable selectivity with Nafion117 (2.20×10^4 S s cm^{-3}) at methanol concentration of 2 mol L^{-1} and higher selectivities than Nafion117 in the rest of the whole range of higher methanol concentration under study (2–12 mol L^{-1}). It is worth noting that the CS–SO_3HY (10%) membrane has the highest selectivity (β from 2.21×10^4 S s cm^{-3} at 2 mol L^{-1} to 4.28×10^4 S s cm^{-3} at 12 mol L^{-1}) among the hybrid membranes, chitosan membrane and Nafion117 owing to its enhanced proton conductivity and lowered methanol permeability. The effect of zeolite content on the selectivity is illustrated in Fig. 13. When the zeolite loading is less than 40%, the selectivity of CS–NaY and CS–H_2NY hybrid membranes keeps almost constant. As the zeolite content goes higher than 40%, the selectivity decreases due to the worse barrier properties caused by poor dispersion of zeolites in the membrane. The CS–HO_3SY membrane with a zeolite content of 40% has the highest selectivity (2.3×10^4 S s cm^{-3} at 2 mol L^{-1}, 5.3×10^4 S s cm^{-3} at 12 mol L^{-1}, the latter being 3.1-fold higher than Nafion117 under the identical condition).

4. Conclusions

NaY zeolite was modified using silane-coupling agents (APTES and MPTMS) and then incorporated into chitosan bulk to fabricate a methanol barrier proton conductive membrane for DMFC. An improved organic–inorganic interfacial morphology was obtained by creating a transitional phase between the polymer and the zeolite particle, leading to reduced methanol permeation. The CS–HO_3SY membranes presented more resistance to methanol crossover than CS–H_2NY and CS–NaY membranes. Although their proton conductivity was lower than that of Nafion117, higher selectivity index ($\beta = \sigma/P$) was obtained for the hybrid membranes, especially at higher methanol concentrations. Furthermore, the CS–HO_3SY membranes showed higher selectivity than Nafion117 in the involved methanol concentration range (2–12 mol L^{-1}) due to the increased proton conductivity arising from the introduction of –SO_3H groups and the increased methanol resistance arising from a better compatibility between organic and inorganic phases. Considering the high selectivity, low cost, environmental benignity as well as facile fabrication, these modified-zeolite-filled chitosan hybrid membranes, CS–HO_3SY membranes in particular, offer an encouraging promise for DMFC development.

Acknowledgements

The authors acknowledge the support from the Programme of Introducing Talents of Discipline to Universities (no.: B06006) and the Cross-Century Talent Raising Program of Ministry of Education of China, the program for Changjiang scholars and innovative research team in University (PCSIRT). We thank Professor Yuxin Wang for his help in the proton conductivity measurements.

References

[1] X. Ren, M.S. Wilson, S. Gottesfel, J. Electrochem. Soc. 143 (1996) L12–L15.
[2] G.T. Burstein, C.J. Barnett, A.R. Kucernak, K.R. Williams, Catal. Today 38 (1998) 425–437.
[3] A. Heinzel, V.M. Barragan, J. Power Sources 84 (1999) 70–74.
[4] A. Kuver, W. Vielstich, J. Power Sources 74 (1998) 211–218.
[5] M.K. Ravikumar, A.K. Shukla, J. Electrochem. Soc. 143 (1996) 2601–2606.
[6] B. Smitha, S. Sridhar, A.A. Khan, J. Power Sources 159 (2006) 846–854.
[7] D.A. Devi, B. Smitha, S. Sridhar, T.M. Aminabhavi, J. Membr. Sci. 262 (2005) 91–99.
[8] C. Hu, B. Li, R. Guo, H. Wu, Z. Jiang, Sep. Purif. Technol. 55 (2007) 327–334.
[9] P. Shao, R.Y.M. Huang, J. Membr. Sci. 287 (2007) 162–179.
[10] T. Uragami, S. Yamamoto, T. Miyata, Biomacromolecules 4 (2003) 137–144.
[11] P. Mukoma, B.R. Jooste, H.C.M. Vosloo, J. Membr. Sci. 243 (2004) 293–299.
[12] V. Tricoli, N. Carretta, M. Bartolozzi, J. Electrochem. Soc. 147 (2000) 1286–1290.
[13] J. Kerres, W. Cui, R. Disson, W. Neubrand, J. Membr. Sci. 139 (1998) 211–225.
[14] B. Smitha, S. Sridhar, A.A. Khan, Macromolecules 37 (2004) 2233–2239.
[15] M. Yamada, I. Honma, Polymer 46 (2005) 2986–2992.
[16] D. Kima, H. Park, J. Rhim, Y. Lee, J. Membr. Sci. 240 (2004) 37–48.
[17] E.N. Gribov, E.V. Parkhomchuk, I.M. Krivobokov, J.A. Darr, A.G. Okunev, J. Membr. Sci. 297 (2007) 1–4.

[18] V.S. Silva, B. Ruffmann, H. Silva, V.B. Silva, A. Mendes, L.M. Madeira, S. Nunes, J. Membr. Sci. 284 (2006) 137–144.
[19] Y. Kim, J.S. Lee, C.H. Rhee, H.K. Kim, H. Chang, J. Power Sources 162 (2006) 180–185.
[20] Z. Huang, Y. Shi, R. Wen, Y. Guo, J. Su, T. Matsuura, Sep. Purif. Technol. 51 (2006) 126–136.
[21] R. Mahajan, R. Burns, M. Schaeffer, W.J. Koros, J. Appl. Polym. Sci. 86 (2002) 881–890.
[22] R. Mahajan, W.J. Koros, Polym. Eng. Sci. 42 (2002) 1432–1441.
[23] E. Okumu, T. Gurkan, L. Yılmaz, J. Membr. Sci. 223 (2003) 23–38.
[24] W. Yuan, H. Wu, B. Zheng, X. Zheng, Z. Jiang, X. Hao, B. Wang, J. Power Sources 172 (2007) 604–612.
[25] Y. Fu, C. Hu, K. Lee, J. Laic, Desalination 193 (2006) 119–128.
[26] Y. Li, H. Guana, T. Chung, S. Kulprathipanja, J. Membr. Sci. 275 (2006) 17–28.
[27] C. Hu, T. Liu, K. Lee, R. Ruaan, J. Lai, Desalination 193 (2006) 14–24.
[28] S. Ren, G. Sun, C. Li, Z. Liang, Z. Wu, W. Jin, X. Qin, X. Yang, J. Membr. Sci. 282 (2006) 450–455.
[29] Z. Liang, T. Zhao, J. Prabhuram, J. Membr. Sci. 283 (2006) 219–224.
[30] B. Zhan, M.A. White, M. Lumsden, Langmuir 19 (2003) 4205–4210.
[31] H. Wu, Y. Wang, S. Wang, J. New Mater. Electrochem. Sys. 5 (2002) 251–254.
[32] T.M. Salama, I. Othman, M. Sirag, G.A. El-Shobaky, Micropor. Mesopor. Mater. 95 (2006) 312–320.
[33] D. Gomes, J. Roeder, M.L. Ponce, S.P. Nunes, J. Membr. Sci. 295 (2007) 121–129.
[34] P. Kanti, K. Srigowri, J. Madhuri, B. Smitha, S. Sridhar, Sep. Purif. Technol. 40 (2004) 259–266.
[35] X. Chen, H. Yang, Z. Gu, Z. Shao, J. Appl. Polym. Sci. 79 (2001) 1144–1149.
[36] P. Mukoma, B.R. Jooste, H.C.M. Vosloo, J. Power Sources 136 (2004) 16–23.
[37] B.P. Ladewig, R.B. Knott, D.J. Martin, J.C. Diniz da Costa, G.Q. Lu, Electrochem. Commun. 9 (2007) 781–786.
[38] C. Li, G. Sun, S. Ren, J. Liu, Q. Wang, Z. Wu, H. Sun, W. Jin, J. Membr. Sci. 272 (2006) 50–57.
[39] V.V. Binsu, R.K. Nagarale, V.K. Shahi, P.K. Ghosh, React. Funct. Polym. 66 (2006) 1619–1629.
[40] J. Ramırez-Salgado, Electrochim. Acta 52 (2007) 3766–3778.
[41] E. Lopez-Chavez, J.M. Martınez-Magadan, R. Oviedo-Roa, J. Guzman, J. Ramırez-Salgado, J. Marın-Cruz, Polymer 46 (2005) 7519–7527.
[42] B. Libby, W.H. Smyrl, E.L. Cussler, AIChE J. 49 (2003) 991–1001.